Available online at www.sciencedirect.com
SCIENCE DIRECT®
Biochimica et Biophysica Acta 1557 (2003) 83–90
BIOCHIMICA ET BIOPHYSICA ACTA
BBA
www.bba-direct.com

# HiPIP in *Rubrivivax gelatinosus* is firmly associated to the membrane in a conformation efficient for electron transfer towards the photosynthetic reaction centre

Clément Lieutaud[a], Wolfgang Nitschke[b], André Verméglio[c], Pierre Parot[a], Barbara Schoepp-Cothenet[b,*]

[a] *Laboratoire de Biophysique des Transporteurs d'Electrons, Faculté des Sciences de Luminy, 136 Avenue de Luminy, 13288 Marseille Cedex 9, France*
[b] *Laboratoire de Bioénergétique et Ingénierie des Protéines UPR 9036, Institut de Biologie Structurale et Microbiologie, CNRS, 31, Chemin Joseph Aiguier, 13402 Marseille Cedex 20, France*
[c] *CEA/Cadarache DEVM-Laboratoire de Bioénergétique Cellulaire, UMR 163-CNRS-CEA, Univ-Méditerranée CEA1000, 13108 Saint Paul lez Durance Cedex, France*

Received 30 July 2002; received in revised form 11 November 2002; accepted 9 December 2002

**Abstract**

High potential iron-sulfur protein (HiPIP), a small soluble redox protein, has been shown to serve in vivo as electron donor to the photosynthetic reaction centre (RC) in *Rubrivivax gelatinosus* [Biochemistry 34 (1995) 11736]. The results of time-resolved optical spectroscopy on membrane-fragments from this organism indicates that the photooxidized RC is re-reduced by HiPIP even in the absence of the soluble fraction. This implies that a significant fraction of HiPIP can firmly bind to the membrane in a conformation able to interact with the RCs. Salt treatment of the membrane-fragments abolishes these re-reduction kinetics, demonstrating the presence of HiPIP on the membrane due to association with the RC rather than due to simple trapping in hypothetical chromatophores. The existence of such a functional complex in membranes is confirmed and its structure further examined by electron paramagnetic resonance (EPR) performed on membrane-fragments. Orientation-dependent EPR spectra of HiPIP were recorded on partially ordered membranes, oxidized either chemically or photochemically. Whereas hardly any preferential orientation of the HiPIP was seen in the chemically oxidised sample, a subpopulation of HiPIP showing specific orientations could be photooxidised. This fraction arises from the electron transfer complex between HiPIP and the RC.


*Keywords:* High potential iron-sulfur protein; Purple bacterium; Electron transfer complex; EPR; Oriented membrane multilayer

## 1. Introduction

High potential iron-sulfur proteins (HiPIPs) constitute a class of small soluble electron transport proteins found in both photosynthetic [1,2] and nonphotosynthetic [3,4] representatives of the proteobacteria as well as in members of the so-called FBC-group (Flexibacter, Bacteroides, Cytophaga-group) [5]. Whereas HiPIPs from a number of organisms have been studied to great detail with respect to electrochemical properties [6,7], primary sequence [8–13] and three-dimensional structure [14–24] over the last three decades, their functional role in the parent organisms remained elusive until recently.

On the basis of their abundances and their appropriate redox potential, HiPIPs have been proposed to act as alternative electron donors to the purple bacterial photosynthetic reaction centres (RCs) for the species where the usual electron donor cytochrome (cyt) $c_2$ was missing [2]. Time-resolved optical spectroscopy performed on the purple bacterium *Rubrivivax* (*Rv.*) *gelatinosus*, *Rhodoferax* (*Rf.*) *fermentans* and *Rhodocyclus* (*Rc.*) *tenuis* clearly demonstrated that under certain conditions HiPIP acts as the physiological electron shuttle between the cyt $bc_1$ complex

*Abbreviations:* cyt, cytochrome; DAD, 2,3,4,5-tetramethyl-*p*-phenylenediamin; EPR, electron paramagnetic resonance; $E_m$, redox midpoint potential; HiPIP, high potential iron-sulfur protein; MOPS, 3-(*N*-morpholino)propanesulfonic acid; P, special pair; RC, reaction centre

* Corresponding author. Tel.: +33-4-91164672; fax: +33-4-91164578.
*E-mail address:* schoepp@ibsm.cnrs-mrs.fr (B. Schoepp-Cothenet).

0005-2728/02/$ - see front matter © 2002 Elsevier Science B.V. All rights reserved.
doi:10.1016/S0005-2728(02)00397-3

and the RC-associated tetraheme cyt subunit [25–28]. A subsequent screening of photosynthetic proteobacteria using this technique showed that HiPIP participates in photosynthetic electron transport in most species of purple bacteria containing a tetraheme subunit [29]. Under aerobic conditions, HiPIP appears to transport electrons from the cyt $bc_1$ complex to the terminal oxidase in *Rf. fermentans* [26], *Rhodospirilum salinarum* [30], and *Rhodothermus marinus* [31].

Analysis of flash-induced absorption changes as a function of the relative concentration of RC and HiPIP suggested the formation of a complex between both components during photosynthetic electron transfer [25,27]. This association may be governed by electrostatic interactions as suggested by the results of salt treatments [25,27]. In the present work the structural characteristics of this complex were studied in more detail by flash-induced absorption change spectroscopy and electron paramagnetic resonance (EPR) on oriented and non-oriented membranes in *Rv. gelatinosus*. Our results suggest that HiPIP may be bound to the tetraheme subunit as a dimer.

## 2. Experimental procedures

### 2.1. Bacterial growth and preparation of membrane fragments

Cultures of *Rv. gelatinosus* (IL144-wild type) were grown anaerobically at 30 °C under continuous illumination (75 μmol photons $m^{-2}$ $s^{-1}$) in Hutner medium (containing minerals, chelating agents, growth factors, malate, glutamate, and acetate [32]). Membrane fragments were prepared as reported by Nitschke et al. [33]. Oriented membrane multilayers were obtained by partial dehydration on mylar following the method described by Rutherford and Sétif [34]. In order to obtain ascorbate-reduced and ferricyanide-oxidised oriented samples, diluted (1:50) samples of membrane fragments were pretreated by addition of 5 mM ascorbate and 2 mM ferricyanide, respectively (both in the presence of 50 mM MOPS, pH 7.0), sedimented by ultracentrifugation, and washed in distilled water. When needed, further reduction or oxidation of the membrane-fragments was obtained by dipping the membrane multilayers in a solution containing 2 mM sodium hexachloroiridate (IV) or 5 mM ascorbate followed by rapid redrying under a stream of argon gas.

### 2.2. Light-induced absorption changes

Membrane fragments were diluted in 10 mM Tris–HCl buffer (pH 7). Xenon flash-induced absorption changes were recorded with a laboratory-built spectrophotometer as described previously [25]. Duration of the actinic flash is about 10 μs.

### 2.3. EPR spectroscopy

EPR spectra were recorded using a Bruker ESP 300 X-band spectrometer fitted with an Oxford Instruments liquid Helium cryostat and temperature control system. Illumination in the EPR cavity was carried out by using a slide projector providing 2000 μE $m^{-2}$ $s^{-1}$ of white light at the EPR cavity window after being filtered through 2 cm of water to remove infrared radiation. During illumination at room temperature, the EPR tube containing oriented membranes was kept in a water/ice bath in order to minimize heating of the sample.

## 3. Results

### 3.1. Light-induced absorption changes

Flash excitation of membranes of *Rv. gelatinosus* IL144, poised at potentials where only high potential hemes are reduced (by 20 μM ascorbate/20 μM DAD treatment), induced the photooxidation of one of the high potential hemes (Fig. 1) monitored at 422 nm. Even in the absence of additional electron donor, 70% of the photooxidized high potential heme, as measured in the Soret band, is re-reduced with a half-time of 500 ms (Fig. 1, closed squares). Spectra recorded in the α-band during re-reduction of the oxidised high potential hemes do not show any shift of the α-band (results not shown). Two hypothesis could explain this re-reduction. First, it is due to back-reaction from $Q_B^-$ to the oxidised high potential heme. The second hypothesis is that, even in the absence of soluble diffusing electron donor, the oxidised high potential heme is re-reduced by a secondary electron donor. In order to test the first hypothesis, stigmatellin, an inhibitor of the $Q_A$–$Q_B$ electron transfer [35], was added. Presence of the inhibitor had no effect on the re-reduction phase (results not shown). This experiment rules out the possibility of charge recombination between $Q_B^-$ and the oxidised high potential heme. To test the second hypothesis, we have performed salt treatments. Addition of 100 mM NaCl completely abolished the fast phase of re-reduction of the photooxidised high potential heme (Fig. 1, closed triangles) whereas 50 mM NaCl reduced its amplitude by 19% without affecting the halftime (Fig. 1, closed circles). These results indicate salt destabilisation of a preformed complex between the tetraheme cyt and a non-heme secondary electron carrier. Since HiPIP is known to be the major electron donor to the cyt subunit in *Rv. gelatinosus* cells under most physiological conditions, it is tempting to assume that the non-heme secondary electron donor in isolated membranes also corresponds to this iron-sulfur protein.

### 3.2. EPR on non-oriented membrane fragments

Since HiPIP has only relatively weak optical absorption bands, EPR spectroscopy was used to assay the presence of

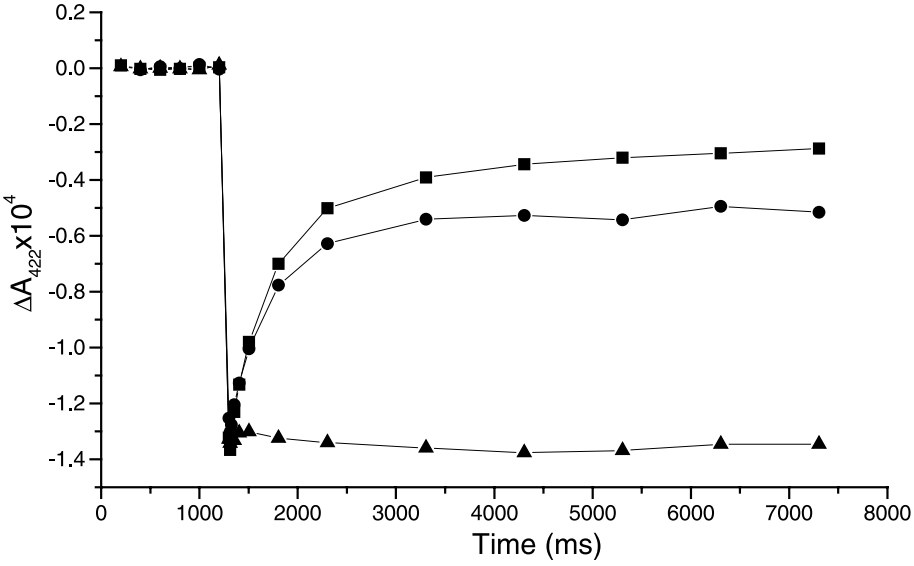


Fig. 1. Kinetics of High Potential hemes re-reduction (xenon flash excitation) measured at 422 nm on membrane fragments in the absence (squares) or in presence of 50 mM NaCl (circles) or 100 mM NaCl (triangles). Membrane fragments (390 nM of RC) were placed in the presence of 20 μM ascorbate/20 μM DAD to achieve the reduction of the High Potential hemes while maintaining the Low Potential hemes in the oxidised state.

HiPIP bound to membranes of *Rv. gelatinosus*. Fig. 2 shows EPR spectra recorded on oxidised membrane fragments. The sample was oxidised by the addition of 2 mM sodium hexachloroiridate (IV). The $g_z$-peaks of the RC-associated cyt subunit [33] could be discerned in the field region of 180 to 230 mT on the spectrum taken on a wide scan but this spectrum was largely dominated by the signals of oxidised HiPIP in the field region between 310 and 340 mT, confirming that this soluble electron carrier protein has a sufficiently high affinity for the membrane to co-sediment during an ultracentrifugation step (spectra a). The spectra shown in the inset represent the HiPIP signal recorded under conditions more appropriate for this specific paramagnetic centre. Salt treatment of these membranes almost completely abolished the spectrum due to HiPIP (Fig. 2, spectra b). These results confirm the hypothesis of a strong affinity

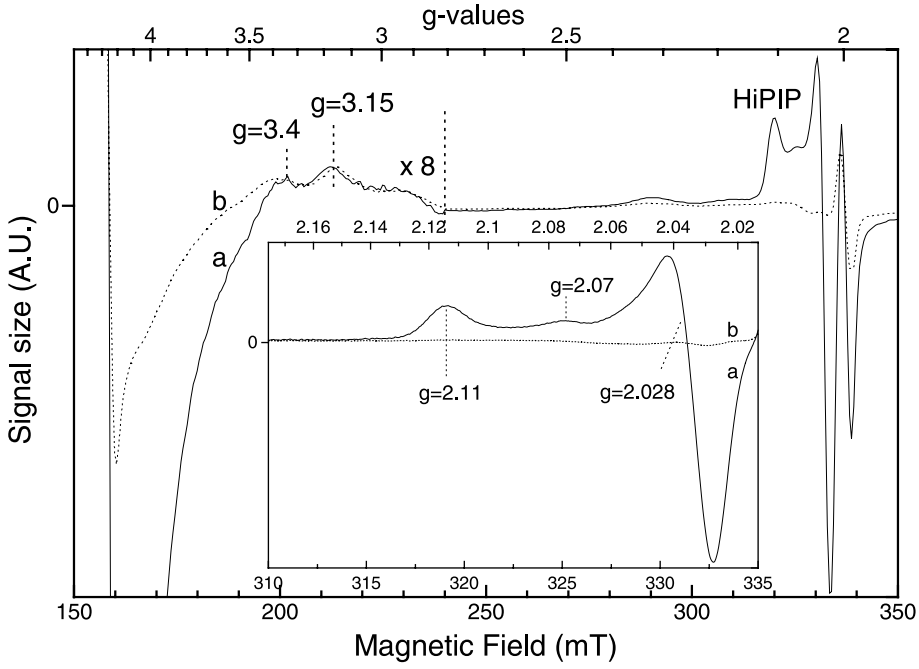


Fig. 2. EPR spectra of oxidised membrane-fragments from *Rv. gelatinosus*. Natives membranes (spectra a) or 100 mM NaCl-treated membranes (spectra b) were oxidised by addition of 2 mM ferricyanide, 20 mM MOPS (pH 7.0), diluted in 20 mM MOPS pH 7.0, sedimented by ultracentrifugation and resuspended in 20 mM MOPS, pH 7.0. Inset: Spectra recorded in the magnetic field region where the signals of the HiPIP are detected. Instrument settings: microwave frequency, 9.44 GHz; temperature, 15 K; microwave power, 6.3 mW (inset: 0.63 mW); modulation, 3.2 mT (inset: 1 mT).

of HiPIP for the membrane which can be destabilised by salt treatment. This excludes the possibility that the observed HiPIP is due to vesicle trapped protein. The spectrum recorded on oxidised, nontreated membrane fragments closely resembles the previously published EPR spectrum of HiPIP obtained on RT-illuminated whole cells of *Rv. gelatinosus* [25]. At least four different components at 2.11, 2.07 and two superimposed lines at 2.028 are visible and the spectrum can therefore not be straightforwardly decomposed into principal *g*-tensor directions. Heterogeneity in the population of HiPIP molecules [36] and heterogeneity in the location of the mixed valence pair within the [4Fe–4S]-cluster [37–41] have alternatively been proposed to explain the composite spectrum (see also Discussion). Reduction of the sample by ascorbate almost completely abolished the spectrum due to HiPIP (data not shown). Illumination at 4 K in the EPR cavity, known to result in stable charge separation between the electron acceptor $Q_A$ and the 300-mV heme of the RC-associated tetraheme subunit in a fraction of centres [33,42], did not induce any oxidation of HiPIP (not shown). By contrast, when the sample was thawed, illuminated at room temperature, and refrozen under illumination, close to 100% of HiPIP were seen to undergo photo-induced oxidation, in agreement with the observations made on whole cells [25].

It is of note that photooxidation of HiPIP in the liquid sample after thawing does not necessarily imply specific recognition between the RC and HiPIP but might simply be due to slow electrochemical equilibration with the photo-induced positive charges on the RC.

### *3.3. Redox potential dependence of the HiPIP EPR-signal in membrane multilayers oriented by partial dehydration*

Fig. 3 shows EPR spectra of HiPIP recorded on partially dehydrated membrane multilayers at different states of reduction before and after illumination with white light at room temperature. For all spectra shown in Fig. 3, the magnetic field was oriented parallel to the plane of the membrane.

The dashed line represents the spectrum taken on samples obtained by drying of ferricyanide-washed membranes. Further oxidation of these membrane samples was obtained by dipping the membranes in a solution containing 2 mM hexachloroiridate followed by rapid redrying under a stream of argon gas (Fig. 3, dotted line). This indicated that part of the population of oxidised HiPIP clusters became re-reduced during the drying procedure. We have systematically observed partial re-reduction of redox centres having $E_m$-values above +300 mV during drying (unpublished observation).

Reduction of the membrane multilayers by dipping in ascorbate and renewed drying essentially abolished the HiPIP spectrum (Fig. 3, dash-dotted line). Subsequent illumination at RT (Fig. 3, continuous line) resulted in photooxidation of 25% of the total signal obtained by chemical oxidation (see above).

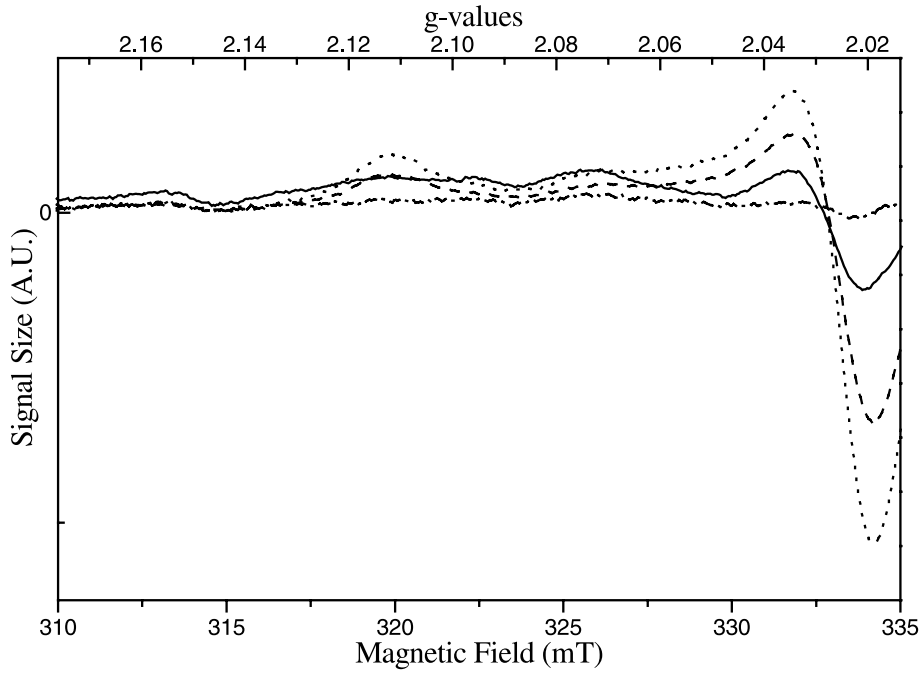


Fig. 3. EPR spectra recorded on partially oriented membrane multilayers from *Rv. gelatinosus*. Spectrum obtained in the ascorbate-reduced state prior to (dash-dotted line) and after (continuous line) illumination at room temperature as well as in the chemically oxidised states achieved by drying of ferricyanide-treated membrane fragments (dashed line) and by subsequent dipping and redrying of already oriented samples in a solution containing 2 mM sodium hexachloroiridate (IV) (dotted line). Instrument conditions were as indicated in Fig. 2 inset.

### 3.4. Orientation dependence of HiPIP EPR spectra

EPR spectra were recorded on oriented hexachloroiridate-oxidised or ascorbate-treated/illuminated membranes from *Rv. gelatinosus* in the range $-40°$ to $+110°$ angle between the magnetic field and the plane of the membrane fragments. Fig. 4 shows representative spectra for the case of the hexachloroiridate oxidised sample (4A) and of the ascorbate treated/illuminated sample (4B).

A pronounced anisotropy was visible in the spectra recorded on the samples reduced by ascorbate and subsequently illuminated at RT, whereas in the chemically oxidised samples, only negligible spectral variations could be discerned. Polar plot evaluations performed on the different signals obtained on the RT-illuminated membranes indicate the presence of two different conformations (see for example the angle dependence of $g=2.11$ for *Rv. gelatinosus* in Fig. 5). On heme centres and [$Fe_2$-$S_2$] clusters, observed

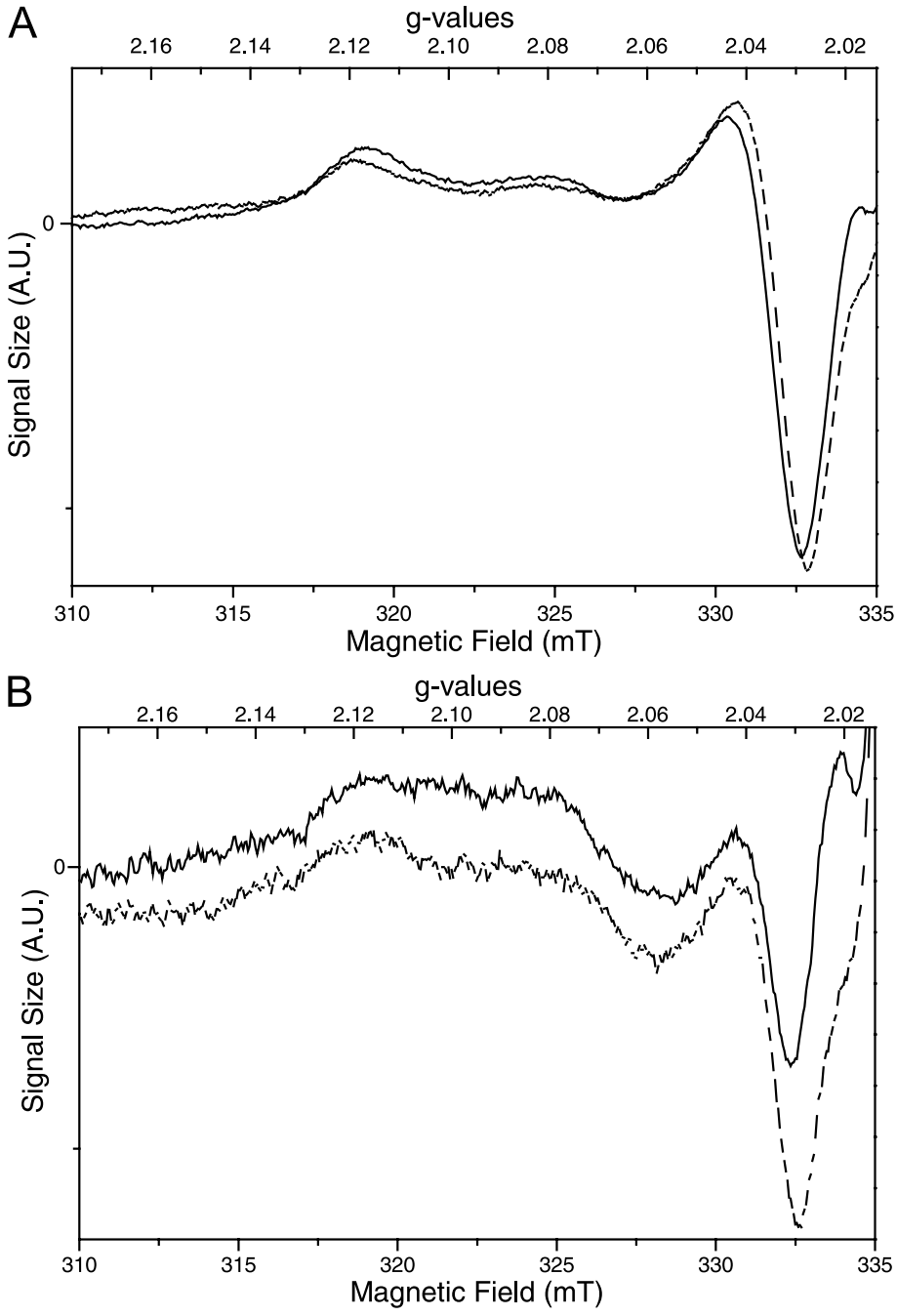


Fig. 4. EPR spectra variations recorded on partially oriented membrane multilayers from *Rv. gelatinosus*. Maximal variations in spectra obtained for the ascorbate-reduced samples after illumination at room temperature (A) as well as for the chemically oxidised states (achieved by drying of ferricyanide-treated membrane fragments, (B) are illustrated by selected spectra.

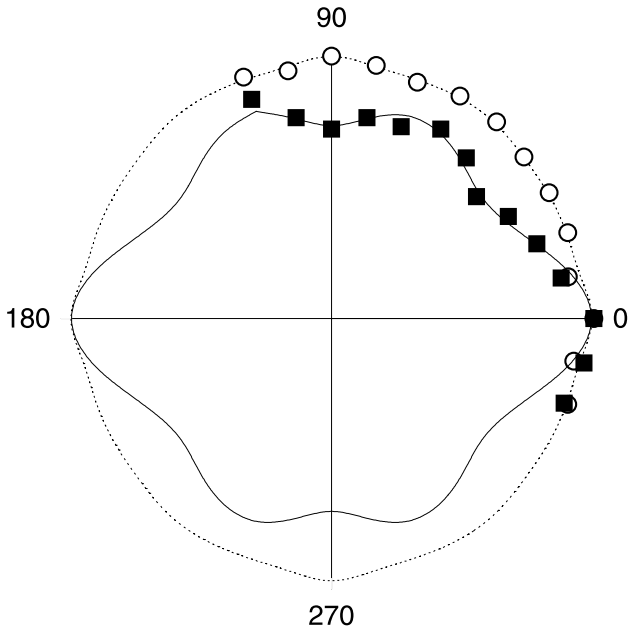


Fig. 5. Polar plot of the dependence of the $g_z = 2.11$ signal amplitude vs. angle of the magnetic field with respect to the membrane plane in the case of *Rv. gelatinosus*. Filled symbols denote data points taken on the ascorbate-reduced sample after illumination and open symbols mark experiments performed on the sodium hexachloroiridate (IV)-oxidised state.

orientations of EPR signals can be directly converted into structural information with respect to geometry of these redox centres. Unfortunately, however, neither the identification of signals to *g*-tensor orientations nor the attribution between *g*-tensor principal axes and molecular axes is unambiguously solved for HiPIP proteins at the present time [36,43]. Exploitation of the full information content of the angle-dependence of EPR signals therefore has to await clarification of these issues.

## 4. Discussion

### *4.1. Complex formation between the HiPIP and the tetraheme*

As shown above, a significant fraction of HiPIP protein present in cells of *Rv. gelatinosus* co-sedimented with the membrane during ultracentrifugation. It is of note that due to the tubular structure of membrane invaginations in *Rv. gelatinosus* [44], French press treatment does not produce closed vesicles (chromatophores) in this bacterium. We have verified this for our case by electron microscopy (not shown). The result of the salt treatment experiment furthermore rules out the explanation of the presence of HiPIP in membrane fragments by formation of such vesicles. The strong anisotropy of EPR signals of the photooxidised HiPIP (see above) demonstrates that a fraction of HiPIP is firmly bound to the membranes (via the tetraheme subunit).

Under aerobic conditions, both high potential hemes of the tetraheme subunit were seen to be reduced after a short period (about 1 min) of dark incubation in *Rv. gelatinosus* [25]. After photooxidation of the RC, HiPIP was found to serve as the electron donor to the RC. Incubation under anaerobic condition resulted in additional reduction of the low potential pair of hemes in the tetraheme subunit. Under these latter conditions, however, electron donation from HiPIP required two pre-flashes oxidising the low potential hemes [25]. The ascorbate-reduced oriented samples used in the EPR study and the ascorbate/DAD-reduced samples used in the kinetic study correspond to the state where HiPIP acts as the predominant electron donor to the photooxidised tetraheme subunit. Therefore, the phenomena observed in our experiments arise from physiological electron transfer complexes between HiPIP and the RC.

A fraction (25–30% as judged by EPR signal size) of the membrane-associated HiPIPs could be photooxidised at room temperature by the photosynthetic RC in partially dehydrated oriented membrane multilayers. Since diffusion of soluble components cannot occur in these immobilised samples, the HiPIP molecules undergoing photooxidation had to be present in a preformed electron transfer complex with the tetraheme cyt subunit of the RC prior to drying.

This result is in agreement with the kinetics of electron transfer between HiPIP and the photooxidised tetraheme subunit obtained at RT with membrane-fragments without addition of any soluble fraction. As judged from re-reduction kinetics of hemes measured optically on membrane fragments of *Rv. gelatinosus*, between 10% [25] and 70% [this work] of the total amount of photosynthetic RCs contained associated HiPIP molecules. In the work of Schoepp et al. [25], the small phase (10%) of heme re-reduction was not taken into account and the results were therefore interpreted to indicate virtual absence of HiPIP from the membrane fraction. The data shown above clearly demonstrate that a substantial amount of HiPIP is bound to the membrane with the fraction of molecules competent to donate being somewhat variable but always observable. The parameters explaining the large difference between the data published previously [25] and our present results are not clear so far. In line with the presence of such preformed complexes, photooxidised HiPIP gave rise to strongly anisotropic EPR spectra indicating distinct conformations.

The remaining 70–75% of HiPIP molecules (observed in the EPR experiments), that were fixed to the membrane but that were not photooxidised by the RC can arise from the following populations: (a) HiPIP molecules that were associated to the RC albeit in conformations that did not permit electron donation to the tetraheme cyt, (b) HiPIP molecules that were associated to RCs containing a damaged electron acceptor system resulting in rapid recombination of the charge-separated pair of charges and thereby precluding electron donation from the tetraheme cyt to $P^+$, (c) HiPIP molecules associated with the cyt $bc_1$ complex, an oxidase or unspecifically bound to the membrane.

### 4.2. Identity of the binding site on the tetraheme subunit

Based on alterations of in vitro electron transfer between HiPIP and the tetraheme subunit induced by site-directed mutagenesis of surface-exposed residues, Osyczka et al. [45,46] have concluded that HiPIP probably binds at the distal top of the tetraheme subunit close to the low potential heme 1.

The finding of the presence of at least two populations of differently oriented HiPIP molecules photooxidised by the RC can be interpreted in three different ways:

(a) The tetraheme subunit contains two distinct binding sites for HiPIP.
(b) A putative unique binding site can accommodate two distinct binding conformations of HiPIP.
(c) Rather than a monomeric HiPIP, it is a dimer of HiPIP molecules that binds to unique interaction site. This possibility is suggested by the observation that the large majority of HiPIP molecules from different species crystallize as dimers and that HiPIP frozen in the presence of salt may exist in dimeric form [36,47].

Mutagenesis studies by Osyczka et al. [45,46] suggested the presence of a unique interaction site for HiPIP close to the low potential heme 1 of the tetraheme subunit. These data strongly argue against the first scenario. At the time being, we cannot decide between the two latter possibilities. Scheme 1 shows possible docking models able to rationalise all experimental data on *Rv. gelatinosus* presently available (Scheme 1). In the framework of this model, the reduced HiPIP (either in two different conformations or as a dimer) would form a relatively tight complex with the tetraheme subunit by docking at a site close to the low potential heme 1. At moderately reducing conditions, i.e. the high potential pair of hemes reduced and the low potential pair of hemes oxidised, flash-oxidation of the special pair (P) would abstract an electron from the high potential pair of hemes. The bound HiPIP would then re-reduce the oxidised high potential heme via electron transfer through oxidised low potential heme.

For the case of the fully reduced tetraheme cyt, flash oxidation will result in oxidation of a low potential heme that is not able to abstract an electron from the significantly more oxidant HiPIP molecules just as is observed in vitro and in vivo (see above). Two consecutive turnovers of the RC are necessary to oxidise the low potential pair of hemes and allow electron abstraction from HiPIP upon subsequent turnovers [25]. It is noteworthy that recent results by Masuda et al. [48] on cytochrome subunit from the purple bacterium *Rhodovulum sulfidophilum* demonstrate the absence of the most distal low potential heme 1, proposed as electron entry site in *Rv. gelatinosus* and *B. viridis* [46,49]. Since soluble cytochrome $c_2$ is able to reduce the RC via this cytochrome subunit [50], at least for the case of this specific bacterium, binding site(s) close to one of the other three hemes must exist. This also resuscitates speculations about alternative binding sites on all RC-associated tetraheme subunits.

Unfortunately, the lack of a conclusive attribution between EPR signals and *g*-tensor orientations for HiPIP precludes our orientation data to be converted into structural information. Once the required information is available, the conformation of HiPIP with respect to the tetraheme subunit

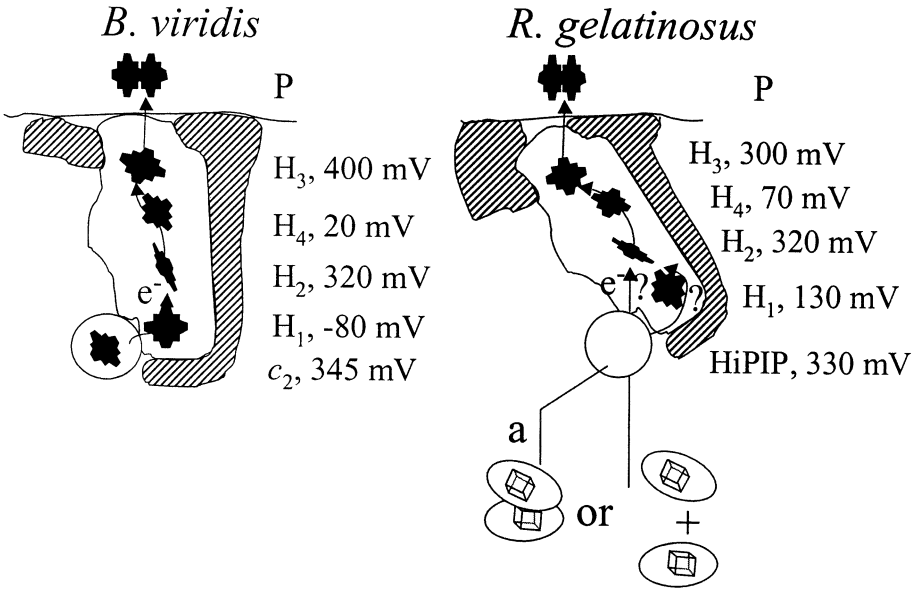


Scheme 1. Schematic representation of docking and electron transfer models in the cases of *B. viridis* and *Rv. gelatinosus* . In the case of *B. viridis*, kinetic data [49] show that the electron transfer from the soluble cyt $c_2$ to the high potential occurs via the reduction of the low potential heme 1 close to which the cyt $c_2$ is docked. The docking model presented here for *Rv. gelatinosus*, incorporating results from mutagenesis studies [45], kinetic data on whole cells [25] and the EPR results presented here, proposes a similar electron transfer pathway.

will be deduced, possibly helping to solve the question of the uniqueness of the binding site.

## References


[1] R.G. Bartsch, Biochim. Biophys. Acta 1058 (1991) 28–30.
[2] T.E. Meyer, in: R.E. Blankenship, M.T. Madigan, C.E. Bauer (Eds.), Anoxygenic Photosynthetic Bacteria, Kluwer Academic Publishing, Dordrecht, 1995, pp. 775–805, Chapter 36.
[3] S.M. Tedro, T.E. Meyer, M.D. Kamen, J. Biol. Chem. 252 (1977) 7826–7833.
[4] C. Cavazza, B. Guigliarelli, P. Bertrand, M. Bruschi, FEMS Microbiol. Lett. 130 (1995) 193–200.
[5] M.M. Peireira, A.M. Antunes, O.C. Nunes, M.S. da Costa, N.M. Teixeira, FEBS Lett. 352 (1994) 327–330.
[6] T.E. Meyer, C.T. Przysiek, J.A. Watkins, A. Bhattacharyya, R.P. Simondsen, M.A. Cusanovich, G. Tollin, Proc. Natl. Acad. Sci. U. S. A. 80 (1983) 6740–6744.
[7] I.A. Mizrahi, T.E. Meyer, M.A. Cusanovich, Biochemistry 19 (1980) 4727–4733.
[8] K. Dus, S. Tedro, R.G. Bartsch, J. Biol. Chem. 248 (1973) 7318–7331.
[9] S.M. Tedro, T.E. Meyer, M.D. Kamen, J. Biol. Chem. 249 (1974) 1182–1188.
[10] S.M. Tedro, T.E. Meyer, M.D. Kamen, J. Biol. Chem. 251 (1976) 129–136.
[11] S.M. Tedro, T.E. Meyer, M.D. Kamen, J. Biol. Chem. 254 (1979) 1495–1500.
[12] S.M. Tedro, T.E. Meyer, R.G. Bartsch, M.D. Kamen, J. Biol. Chem. 256 (1981) 731–735.
[13] S.M. Tedro, T.E. Meyer, M.D. Kamen, Arch. Biochem. Biophys. 241 (1985) 656–664.
[14] C.W. Carter Jr., J. Kraut, S.T. Freer, N.-H. Xuong, R.A. Alden, R.G. Bartsch, J. Biol. Chem. 249 (1974) 4212–4225.
[15] D.R. Breiter, T.E. Meyer, I. Rayment, H.M. Holden, J. Biol. Chem. 266 (1991) 18660–18667.
[16] I. Rayment, G. Wesenberg, T.E. Meyer, M.A. Cusanovich, H.M. Holden, J. Mol. Biol. 228 (1992) 672–686.
[17] L. Banci, I. Bertini, L.D. Eltis, I. Felli, D.H.W. Kastrau, C. Luchinat, M. Piccioli, R. Pierattelli, M. Smith, Eur. J. Biochem. 225 (1994) 703–714.
[18] M.M. Benning, T.E. Meyer, I. Rayment, H.M. Holden, Biochemistry 33 (1994) 2476–2483.
[19] L. Banci, I. Bertini, A. Dikiy, D.H.W. Kastrau, C. Luchinat, P. Sompornpisut, Biochemistry 34 (1995) 206–219.
[20] I. Bertini, A. Dikiy, D.H. Kastrau, C. Luchinat, P. Sompornpisut, Biochemistry 34 (1995) 9851–9858.
[21] I. Bertini, M.M. Couture, A. Donaire, L.D. Eltis, I.C. Felli, C. Luchinat, M. Piccioli, A. Rosato, Eur. J. Biochem. 241 (1996) 440–452.
[22] C. Kerfeld, A.E. Salmeen, T.O. Yeates, Biochemistry 37 (1998) 13911–13917.
[23] E. Parisini, F. Capozzi, P. Lubini, V. Lamzin, C. Luchinat, G. Sheldrick, Acta Crystallogr., D 55 (1999) 1773–1784.
[24] T. Nogi, I. Fathir, M. Kobayashi, T. Nozawa, K. Miki, Proc. Natl. Acad. Sci. U. S. A. 97 (2000) 13561–13566.
[25] B. Schoepp, P. Parot, L. Menin, J. Gaillard, P. Richaud, A. Verméglio, Biochemistry 34 (1995) 11736–11742.
[26] A. Hochkoeppler, P. Kofod, D. Zannoni, FEBS Lett. 375 (1995) 197–200.
[27] A. Hochkoeppler, D. Zannoni, S. Ciurli, T.E. Meyer, M.A. Cusanovich, G. Tollin, Proc. Natl. Acad. Sci. U. S. A. 93 (1996) 6998–7002.
[28] L. Menin, B. Schoepp, P. Parot, A. Verméglio, Biochemistry 36 (1997) 12183–12188.
[29] L. Menin, J. Gaillard, P. Parot, B. Schoepp, W. Nitschke, A. Verméglio, Photosynth. Res. 55 (1998) 343–348.
[30] P. Bonora, I. Principi, B. Monti, S. Ciurli, D. Zannoni, A. Hochkoepler, Biochim. Biophys. Acta 1410 (1999) 51–60.
[31] M.M. Pereira, J.N. Carita, N.M. Teixeira, Biochemistry 38 (1999) 1276–1283.
[32] R.K. Clayton, Biochim. Biophys. Acta 37 (1960) 503–512.
[33] W. Nitschke, I. Agalidis, A.W. Rutherford, Biochim. Biophys. Acta 1100 (1992) 49–57.
[34] A.W. Rutherford, P. Sétif, Biochim. Biophys. Acta 1019 (1990) 128–132.
[35] W. Oettmeier, D. Godde, B. Kunze, G. Höfle, Biochim. Biophys. Acta 807 (1985) 216–219.
[36] W.R. Dunham, W.R. Hagen, J.A. Fee, R.H. Sands, J.B. Dunbar, C. Humblet, Biochim. Biophys. Acta 1079 (1991) 253–262.
[37] B.C. Antanaitis, T.H. Moss, Biochim. Biophys. Acta 405 (1975) 262–279.
[38] L. Banci, I. Bertini, S. Ciurli, S. Ferretti, C. Luchinat, M. Piccioli, Biochemistry 32 (1993) 9387–9397.
[39] J.G. Huber, J.-M. Moulis, J. Gaillard, Biochemistry 35 (1996) 12705–12711.
[40] A.W.E. Dilg, G. Mincione, K. Achterhold, O. Iakovleva, M. Mentler, C. Luchinat, I. Bertini, F.G. Parak, J. Biol. Inorg. Chem. 4 (1999) 727–741.
[41] A.W.E. Dilg, F. Capozzi, M. Mentler, O. Iakovleva, C. Luchinat, I. Bertini, F.G. Parak, J. Biol. Inorg. Chem. 6 (2001) 232–246.
[42] P.L. Dutton, Biochim. Biophys. Acta 226 (1971) 63–80.
[43] R. Kappl, S. Ciurli, C. Luchinat, J. Hüttermann, J. Am. Chem. Soc. 121 (1999) 1925–1935.
[44] H.G. Trüper, J.F. Imhoff, in: A. Balows, H.G. Trüper, M. Dworkin, W. Harder, H.-H. Schleifer (Eds.), The Prokaryotes. A Handbook on the Biology of Bacteria: Ecophysiology, Isolation, Identification, Applications, 2nd ed., Springer-Verlag, New York, 1992, pp. 2556–2561.
[45] A. Osyczka, K.V.P. Nagashima, K. Shimada, K. Matsuura, Biochemistry 38 (1999) 2861–2865.
[46] A. Osyczka, K.V.P. Nagashima, S. Sogabe, K. Miki, K. Shimada, K. Matsuura, Biochemistry 38 (1999) 15779–15790.
[47] M.M.-J. Couture, M. Auger, F. Rosell, A.G. Mauk, E. Boubour, R.B. Lennox, L.D. Eltis, Biochim. Biophys. Acta 1433 (1999) 159–169.
[48] S. Masuda, M. Yoshida, K.V.P. Nagashima, K. Shimada, K. Matsuura, J. Biol. Chem. 274 (1999) 10795–10801.
[49] J.M. Ortega, F. Drepper, P. Mathis, Photosynth. Res. 59 (1999) 147–157.
[50] M. Yoshida, S. Masuda, K.V.P. Nagashima, A. Verméglio, K. Shimada, K. Matsuura, Biochim. Biophys. Acta 1506 (2001) 23–30.